Magn. Reson., 6, 273–279, 2025 https://doi.org/10.5194/mr-6-273-2025 © Author(s) 2025. This work is distributed under the Creative Commons Attribution 4.0 License.





# Long-lived states involving a manifold of fluorine-19 spins in fluorinated aliphatic chains

Coline Wiame, Sebastiaan Van Dyck, Kirill Sheberstov, Aiky Razanahoera, and Geoffrey Bodenhausen

Chimie Physique et Chimie du Vivant (CPCV, UMR 8228), Department of Chemistry, Ecole Normale Supérieure, PSL University, Sorbonne University, CNRS, Paris, 75005, France

**Correspondence:** Kirill Sheberstov (kirill.sheberstov@ens.psl.eu)

Received: 5 June 2025 – Discussion started: 19 June 2025 Revised: 7 October 2025 – Accepted: 7 October 2025 – Published: 24 November 2025

**Abstract.** Long-lived states (LLSs) have lifetimes  $T_{\rm LLS}$  that exceed longitudinal spin-lattice relaxation times  $T_1$ . In this study, lifetimes  $T_{\rm LLS}(^{19}{\rm F})$  have been measured in three different achiral per- and polyfluoroalkyl substances (PFAS) containing two or three consecutive CF<sub>2</sub> groups. In a static magnetic field  $B_0 = 11.7$  T, the lifetimes  $T_{\rm LLS}(^{19}{\rm F})$  exceed the longitudinal relaxation times  $T_1(^{19}{\rm F})$  by about a factor of 2. The lifetimes  $T_{\rm LLS}(^{19}{\rm F})$  can be strongly affected by binding to macromolecules, a feature that can be exploited for the screening of fluorinated drugs. Both  $T_{\rm LLS}(^{19}{\rm F})$  and  $T_1(^{19}{\rm F})$  should be longer at lower fields where relaxation due to the chemical shift anisotropy (CSA) of  $^{19}{\rm F}$  is less effective, which is demonstrated here by running experiments at two fields of 11.7 and 7 T.

# 1 Introduction

The discovery of long-lived states (LLSs) was inspired by spin isomers of dihydrogen (H<sub>2</sub>), in which a non-equilibrium ratio of para- vs. ortho-dihydrogen can persist for many days before relaxing. Many applications of LLSs have been illustrated for pairs of <sup>13</sup>C or <sup>15</sup>N nuclei (Pileio et al., 2012; Feng et al., 2013; Stevanato et al., 2015; Elliott et al., 2019; Sheberstov et al., 2019b), for pairs of <sup>1</sup>H nuclei (Franzoni et al., 2012; Kiryutin et al., 2019a), (less frequently) for pairs of <sup>19</sup>F nuclei (Buratto et al., 2016), for <sup>31</sup>P (Korenchan et al., 2021), and for <sup>103</sup>Rh spins (Harbor-Collins et al., 2024). The slow decays of LLSs have been exploited for the determination of small diffusion coefficients (Cavadini et al., 2005), for measurements of slow chemical exchange (Sarkar et al., 2007), for the storage of hyperpolarization (Vasos et al., 2009; Pileio et al., 2012; Kiryutin et al., 2019b), for investigations of weak ligand-protein binding (Salvi et al., 2012), and for studies of tortuosity in porous media (Dumez et al., 2014; Pileio et al., 2015; Pileio and Ostrowska, 2017; Tourell et al., 2018; Melchiorre et al., 2023). Another application of LLSs is spectral editing, in particular for filtering of selected signals in proteins (Mamone et al., 2020; Sicoli et al., 2024).

# 1.1 Fluorinated drugs

Many drugs contain one or more fluorine atoms since pharmacokinetic studies have shown that their lifetimes in vivo are favored because C-F bonds are harder to break down by enzymes than C-H bonds (Shah and Westwell, 2007). Positron emission tomography (PET) with <sup>18</sup>F-labeled radioligands is widely applied in diagnosis and in drug development (Nerella et al., 2022). Fluorinated drugs also have the advantage of being easy to track by NMR and MRI, since the sensitivity of <sup>19</sup>F NMR is comparable to that of <sup>1</sup>H NMR, while signal overlap is significantly reduced due to the greater chemical shift dispersion, and spectral quality is improved because of the absence of background signals, e.g., water signal (Buchholz and Pomerantz, 2021). For drug screening, it is important to achieve the best possible contrast between the response of a ligand L that binds to a target protein P and a molecule that fails to do so. An LLS involving two or more <sup>19</sup>F spins in a ligand can lead to a remarkable contrast upon binding to a protein target (Buratto et al., 2016). For ligands that bind to a target protein, contrast in <sup>19</sup>F NMR arises from the combined effects of binding on the chemical shifts, on the reduction of symmetry when achiral ligands bind to chiral targets, and on the correlation times of rotational diffusion. The latter effect leads to line broadening by homogeneous transverse  $T_2$  relaxation. In addition, chemical exchange in the intermediate regime can also contribute to line broadening (Buchholz and Pomerantz, 2021). The latter two effects can be distinguished by comparing Carr–Purcell–Meiboom–Gill (CPMG) echo trains with high repetition rates and slow CPMG echo trains using so-called "perfect echoes". The first type of experiment will suppress echo modulations due to homonuclear scalar couplings  $^nJ(^{19}F, ^{19}F)$  and inhibit echo decays due to intermediate exchange (Takegoshi et al., 1989; Aguilar et al., 2012), while the second type of experiment eliminates the effects of  $^nJ(^{19}F, ^{19}F)$  couplings while retaining the effects of intermediate exchange (Lorz et al., 2025).

## 1.2 Long-lived states

In a pair of two spins A and A', the difference between the population of the singlet state  $p(S_0^{AA'})$  and the mean population of the three triplet states  $p(T^{AA'}) =$  $\frac{1}{3}\left(p\left(T_{+1}^{AA'}\right)+p\left(T_{0}^{AA'}\right)+p\left(T_{-1}^{AA'}\right)\right)$  is known as triplet singlet population imbalance, which is immune to relaxation driven by intra-pair dipole-dipole couplings. One speaks of LLSs since these population imbalances decay with lifetimes  $T_{LLS}$  that can greatly exceed  $T_1$  and  $T_2$ . Such a state can be described by a scalar product  $\hat{I}^A$ .  $\hat{I}^{A'}$ , where  $\hat{I}^p = (\hat{I}_x^p, \hat{I}_y^p, \hat{I}_z^p) p \in \{A, A'\}$ . In an achiral aliphatic chain with six spins, denoted as AA'MM'XX' in Pople's notation, one can excite not only two-spin order terms  $\hat{I}^A \cdot \hat{I}^{A'}$  and/or  $\hat{I}^M \cdot \hat{I}^{M'}$  and/or  $\hat{I}^X \cdot \hat{I}^{X'}$  but also four-spin order terms such as  $(\hat{I}^{\hat{M}} \cdot \hat{I}^{\hat{M}'}) \cdot (\hat{I}^{\hat{M}} \cdot \hat{I}^{\hat{M}'})$ and/or  $(\hat{I}^A \cdot \hat{I}^{A'}) \cdot (\hat{I}^X \cdot \hat{I}^{X'})$  and/or  $(\hat{I}^M \cdot \hat{I}^{M'}) \cdot (\hat{I}^X \cdot \hat{I}^{X'})$ . One can also, in principle, excite a six-spin order term,  $(\hat{I}^A \cdot \hat{I}^{A'}) \cdot (\hat{I}^M \cdot \hat{I}^{M'}) \cdot (\hat{I}^X \cdot \hat{I}^{X'})$ , although simulations for protonated aliphatic chains indicate that the yields of such a six-spin term are low (Sonnefeld et al., 2022b). It is challenging to determine separately the coefficients if one excites admixtures of all seven possible products in a six-spin system. Since experiments indicate that the decay constants are often very similar, admixtures of different products tend to relax with an effective mono-exponential decay. These remarks apply to molecules containing either three fluorinated or three protonated methylene groups, including those analyzed in this study and in our previous work on protons (Sonnefeld et al., 2022b).

In many molecules, there are two <sup>19</sup>F spins that have different chemical shifts, e.g., in many difluoro-substituted aromatic rings. In *chiral* molecules containing CF<sub>2</sub> groups, the diastereotopic <sup>19</sup>F nuclei have different chemical shifts if they are not too far from a stereogenic center. In such cases, it is straightforward to excite and observe an LLS involving the two <sup>19</sup>F spins of a CF<sub>2</sub> group. In our labo-

ratory, we often use a sequence of hard pulses developed for this purpose (Sarkar et al., 2007). LLSs have thus been observed in diastereotopic CF<sub>2</sub> groups where their lifetimes  $T_{\rm LLS}$  exceed  $T_1$  significantly (Buratto et al., 2016). In achiral molecules, on the other hand, pairs of <sup>19</sup>F atoms attached to the same carbon are chemically equivalent, i.e., have degenerate chemical shifts, so that the geminal  ${}^2J({}^{19}F, {}^{19}F)$  couplings do not affect the spectra to the first order. Nonetheless, LLS can be excited in such systems provided that the pairs of <sup>19</sup>F atoms are magnetically inequivalent. A pair of <sup>19</sup>F atoms attached to the same carbon atom are magnetically inequivalent if and only if vicinal couplings such as  ${}^3J({}^{19}F,$  $^{19}$ F) or  $^3J(^{19}$ F,  $^1$ H) to  $^{19}$ F or  $^1$ H nuclei in neighboring CF<sub>2</sub> or CH2 groups are not degenerate, i.e., provided that differences such as  $\Delta J_{AM} = J_{AM} - J_{AM'} = J_{A'M'} - J_{A'M}$  and  $\Delta J_{MX} = J_{MX} - J_{MX'} = J_{M'X'} - J_{M'X}$  do not vanish. The degeneracy of vicinal scalar couplings is lifted when the rotamers resulting from rotations about the C-C bonds are not equally populated. This occurs if the potential wells corresponding to the different rotamers have unequal energy.

This work extends the excitation of LLS by spin-lock induced crossing (SLIC; DeVience et al., 2013) to a set of four or six <sup>19</sup>F spins in perfluorinated aliphatic chains of the type –(CF<sub>2</sub>)<sub>n</sub>–. Specifically, we have looked at per- and polyfluoroalkyl (PFAS) molecules, which have been widely studied for their detrimental effects on the environment (Fenton et al., 2021). Studying these molecules and their ability to bind to protein targets could shed more light on their impact on living organisms.

Excitation with a SLIC pulse can also enhance the intensity of outer singlet–triplet (OST) coherences (Sheberstov et al., 2019a), as discussed in more detail below. We have used mono- and polychromatic SLIC, involving the simultaneous application of one, two, or three radio-frequency (RF) fields to one, two, or three multiplets in a <sup>19</sup>F spectrum (Fig. 1), in analogy to our work on <sup>1</sup>H spins in aliphatic chains of the type  $-(CH_2)_n$  (Sonnefeld et al., 2022a, b; Razanahoera et al., 2023; Sheberstov et al., 2024). The resulting long-lived states involve two, four, or six <sup>19</sup>F spins. One must distinguish between two approaches: single- or double-quantum SLIC (SQ- or DQ-SLIC). For DQ-SLIC to be efficient, the RF amplitudes  $\nu_{SLIC}$  of SLIC pulses must be equal to the geminal coupling  $^2J(^{19}F, ^{19}F)$  between two neighboring <sup>19</sup>F spins or twice as large for SQ-SLIC.

A population imbalance between the triplet and singlet states can also be obtained at very low spin temperatures, as may occur in dynamic nuclear polarization (DNP; Tayler et al., 2012; Bornet et al., 2014; Razanahoera et al., 2024). In systems with more than two spins, one can also excite long-lived imbalances between states that belong to different symmetries of the spin permutation group, e.g., an imbalance between populations associated with irreducible representations A and E in CD<sub>3</sub> groups (Kress et al., 2019).

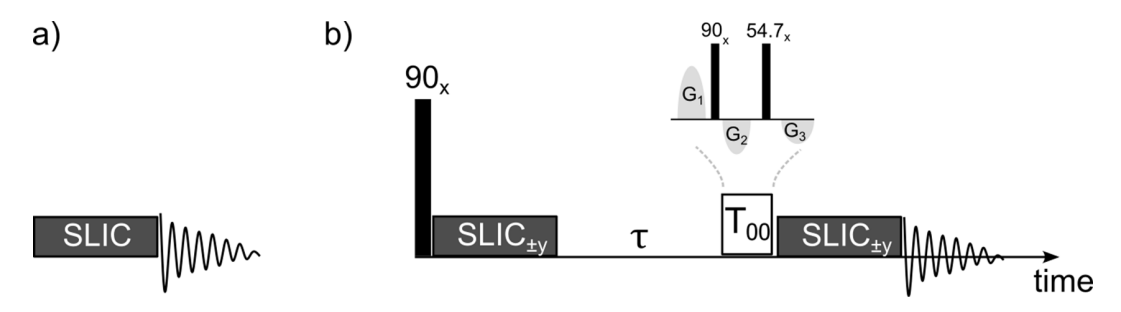


Figure 1. (a) Experiment used to amplify the amplitudes of forbidden "outer singlet–triplet transitions" (OSTs) in conventional <sup>19</sup>F spectra. The radio-frequency (RF) amplitude  $v_{SLIC}$  and duration  $\tau_{SLIC}$  can be optimized empirically to achieve the highest possible OST signal amplitudes (Sheberstov et al., 2019a). (b) Pulse sequence used to study the excitation, relaxation, and reconversion of LLS of <sup>19</sup>F in fluorinated achiral aliphatic chains. The transverse magnetization is excited by a "hard" non-selective  $(\pi/2)_x$  pulse, followed by the application of one, two, or three selective RF fields (polychromatic SLIC pulses) applied simultaneously at the resonance frequencies (chemical shifts) of one, two, or three consecutive CF<sub>2</sub> groups to convert the magnetization into a superposition of various LLS. Two optima result from the level anti-crossings at the single-quantum condition (SQ LAC) or at the double-quantum condition (DQ LAC). The RF amplitudes must be equal to the geminal coupling for DQ LAC, i.e.,  $v_{SLIC}^{DQ} = ^2J(^{19}F, ^{19}F)$  or twice as large for SQ LAC. The maximum efficiency is achieved either for a short pulse duration  $\tau_{SLIC}^{SQ} = 1/\left(\left|\sqrt{2}\Delta J\right|\right)$  for SQ LAC or a longer duration  $\tau_{SLIC}^{DQ} = \sqrt{2}\tau_{SLIC}^{SQ} = 1/\left(\left|\Delta J\right|\right)$  for DQ LAC , where  $\Delta J = (\Delta J_{AM} + \Delta J_{MX})/2$ ,  $\Delta J_{AM} = J_{AM} - J_{AM'} = J_{A'M'} - J_{A'M}$ , and  $\Delta J_{AX} = J_{AX} - J_{AX'} = J_{A'X'} - J_{A'X}$ . After a  $T_{00}$  filter (Tayler, 2020), another set of mono- or polychromatic SLIC pulses allows one to reconvert LLS into observable magnetization.

## 2 Results and discussion

To extend the excitation of LLS from  $^1\text{H}$  to  $^{19}\text{F}$ , a challenge arises from the fact that  $J(^{19}\text{F}_-^{19}\text{F})$  and  $J(^1\text{H}_-^1\text{H})$  differ in the way their magnitude depend on the number of chemical bonds between atoms. Typically, geminal  $^2J(^{19}\text{F}_-^{19}\text{F})$  couplings in CF<sub>2</sub> groups are on the order of 250 to 290 Hz (Krivdin, 2020), much larger than geminal  $^2J(^1\text{H}_-^1\text{H})$  couplings in CH<sub>2</sub> groups, which are about  $\sim -15\,\text{Hz}$ . In  $^1\text{H}$  NMR, typical values of the difference between vicinal couplings lie in the range  $0 < \Delta J(^1\text{H}) < 7\,\text{Hz}$ , while for  $^{19}\text{F}$  NMR, these differences may typically lie in the range  $0 < \Delta J(^{19}\text{F}) < 40\,\text{Hz}$ .

We have explored three achiral fluorinated molecules shown in Fig. 2, selected because the chemical shifts between neighboring  $CF_2$  groups exceed 1 kHz. This means that LLS excitation of a chosen  $CF_2$  group is sufficiently selective, even with RF amplitudes on the order of 250 to 290 Hz for DQ LAC or on the order of 500 to 580 Hz for SQ LAC, so that one can neglect the effects of a SLIC pulse on neighboring  $CF_2$  groups.

## 2.1 Outer singlet-triplet transitions

For the excitation of LLS in aliphatic chains containing  $^{1}$ H (Sonnefeld et al., 2022a), we have estimated the geminal  $^{2}J(^{1}\text{H-}^{1}\text{H})$  couplings and used spin simulation programs (Cheshkov et al., 2018) to optimize the radio-frequency field amplitude  $\nu_{\text{SLIC}}$  and the duration  $\tau_{\text{SLIC}}$ . For  $^{19}\text{F}$ , it is more difficult to estimate all relevant coupling constants. As a consequence of chemical equivalence, the geminal couplings  $^{2}J(^{19}\text{F}, ^{19}\text{F})$  cannot be observed as a splitting but manifest themselves through weakly allowed combination lines that

appear on either side of the <sup>19</sup>F multiplets with intensities that are typically 10<sup>4</sup> times weaker than those of the allowed transitions. The detection of the OST transitions can be improved (Sheberstov et al., 2019a) by irradiating one of the multiplets with a single monochromatic RF field with an amplitude  $v_{rf}$  in the vicinity of the optimum value  $v_{SLIC}$  and a duration near the ideal  $\tau_{SLIC}$  (Fig. 1a). Thus, we were able to enhance the intensities of the OST transitions by up to 2 orders of magnitude. In this work, we have in this manner measured geminal couplings that fall in the range of  $280 < ^2J(^{19}F, ^{19}F) < 295 \text{ Hz}$ . Once the amplitude  $v_{SLIC}$  has been optimized, the duration  $\tau_{SLIC}$  can readily be optimized by searching empirically for the highest signal amplitude. An enhancement of OST transitions can also be achieved using other techniques, such as J-synchronized CPMG (Sheberstov et al., 2019a) or symmetry-based sequences (Sabba et al., 2022).

## 2.2 Lifetimes of long-lived states

The preliminary experiments shown in Fig. 3 allowed us to optimize conditions for SLIC. Using the pulse sequence of Fig. 1b, we observed the decay curves of Fig. 4.

The resulting LLS lifetimes are reported in Table 1. Note that at both fields (11.7 and 7 T), the ratios  $T_{\rm LLS}/T_1$  all lie in the vicinity of 2. We see the pronounced effect of CSA on  $^{19}{\rm F}$  relaxation as both  $T_1$  and  $T_{\rm LLS}$  are longer at a field of 7 T (282.4 MHz for  $^{19}{\rm F}$ ) for molecules PFBS and PFPeA. The ratios  $T_{\rm LLS}/T_1$  remain rather similar at both fields, indicating both  $T_1$  and  $T_{\rm LLS}$  are impacted by relaxation induced by CSA in a similar way. However, a clear trend in the change of  $T_1$  and  $T_{\rm LLS}$  lifetimes measured at the two fields is not seen for PFBA. Fluorinated CF3 methyl groups do not con-

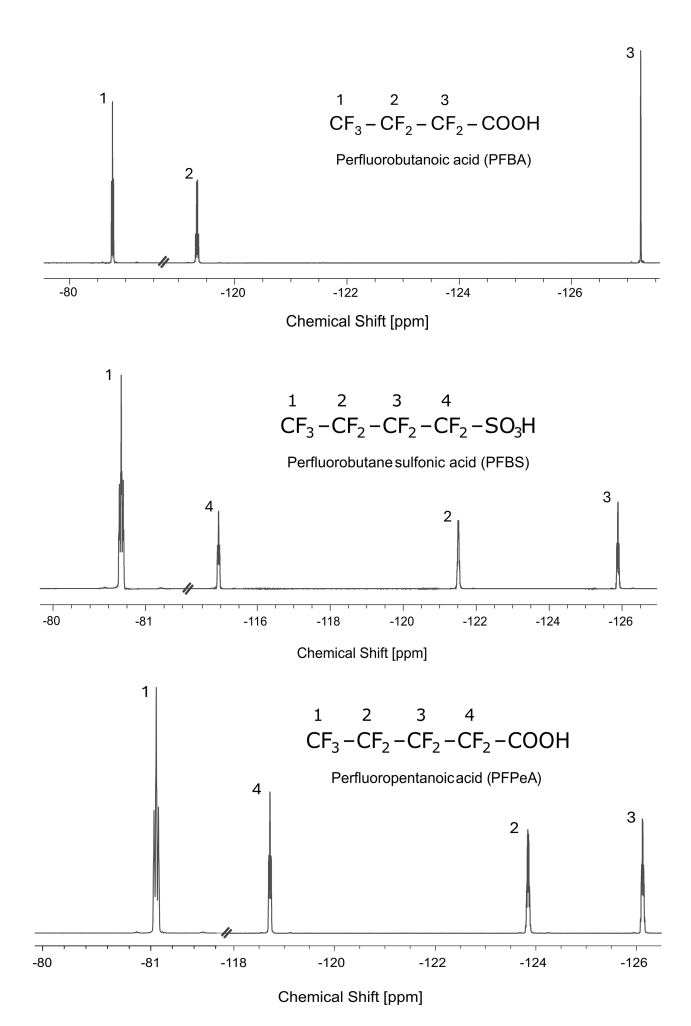


**Figure 2.** Three achiral molecules with fluorinated aliphatic chains studied in this work: perfluorobutanoic acid (PFBA), perfluorobutane sulfonic acid (PFBS), and perfluoropentanoic acid (PFPeA). All three molecules were dissolved in DMSO-d6 at 500 mM concentrations. The spectra were acquired at 298 K on a Bruker WB spectrometer at 11.7 T (470.46 MHz for <sup>19</sup>F, 500 MHz for <sup>1</sup>H) equipped with a NEO console.

tribute to the LLS, as proven by selective decoupling at their resonance frequencies, which affects neither the efficiency of LLS excitation of CF<sub>2</sub> groups nor their lifetimes.

#### 2.3 Protein-ligand titration of PFBS with BSA

It has been previously reported that PFAS have a binding affinity for various proteins (Zhao et al., 2023). To evaluate the ability of  $^{19}\mathrm{F}$  LLS to provide contrast between a free and a bound form, when interacting with a protein, we explored the binding of PFBS to the protein bovine serum albumin (BSA) by measuring the  $T_{\rm LLS}$  of samples with [PFBS] = 50 mM and various concentrations of  $0 < [\mathrm{BSA}] < 100\,\mu\mathrm{M}$ . The contrast can be defined as usual by  $C_1 = (R_1^{\mathrm{obs}} - R_1^{\mathrm{free}})/R_1^{\mathrm{obs}}$  for experiments measuring

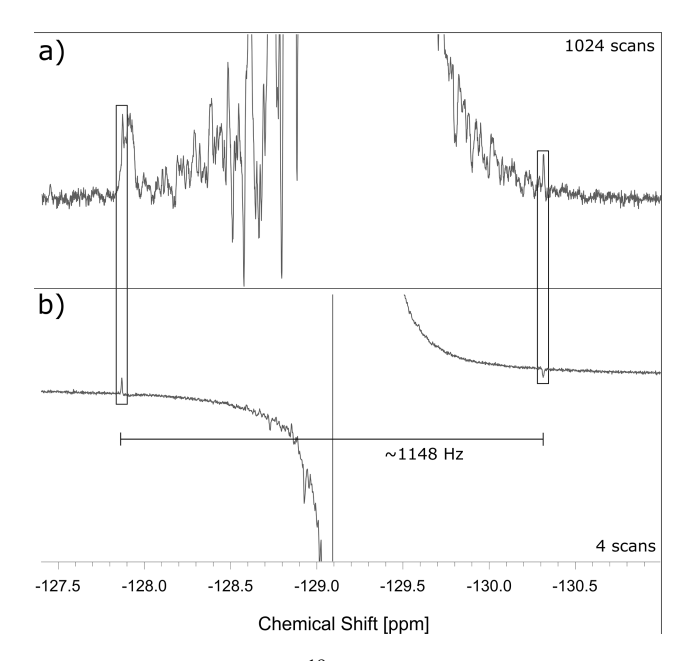


**Figure 3.** (a) Conventional <sup>19</sup>F spectrum at 11.7 T (470.46 MHz for <sup>19</sup>F) of the multiplet of the low-frequency CF<sub>2</sub> group (peak 3 in Fig. 2) of 6.9 M perfluorobutanoic acid (PFBA) in DMSO-d6. The weakly allowed combination lines, known as outer singlet–triplet transitions (OSTs), are emphasized by rectangular frames but cannot be reliably identified as such on the grounds of the top spectrum alone. (b) The OSTs were enhanced by irradiation with an RF field with an amplitude of  $v_{\rm SLIC} = 574$  Hz, applied to the center of the low-frequency CF<sub>2</sub> group in PFBA during  $\tau_{\rm SLIC}$  50 ms, immediately followed by the observation of the <sup>19</sup>F free induction decay (i.e., without conversion into LLS). The frequency difference between the two framed transitions is 1148 Hz, which corresponds to four times <sup>2</sup>  $J(^{19}F^{-19}F)$ . The top spectrum required 1024 scans, while the bottom spectrum was obtained with only four scans.

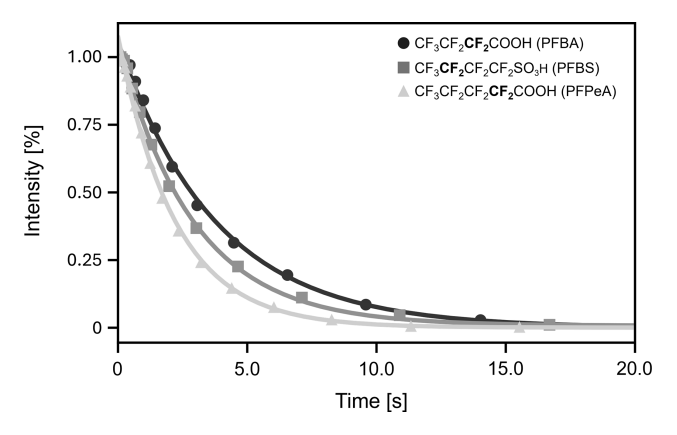


**Figure 4.** Decays of LLS (actually admixtures of two-, four-, and minor amounts of six-spin order LLS terms) for three different fluorinated molecules at 11.7 T (470.46 MHz for <sup>19</sup>F). The decays were fitted with mono-exponential functions to determine the LLS lifetimes reported in Table 1. The CF<sub>2</sub> groups for which the decays are shown are highlighted in bold in the molecular formulae.

**Table 1.** Optimized radio-frequency field amplitude  $v_{\rm SLIC}$  and optimized duration  $\tau_{\rm SLIC}$  for spin-lock induced crossing (SLIC) to generate long-lived states involving four or six  $^{19}{\rm F}$  spins of the fluorinated aliphatic chains, using two or three RF fields applied simultaneously to the two or three multiplets of the three fluorinated molecules (Fig. 2) at 11.7 T (470.46 MHz for  $^{19}{\rm F}$ ) and 7 T (282.4 MHz for  $^{19}{\rm F}$ ). The spin-lattice relaxation times  $T_{\rm LLS}$  were determined by the inversion-recovery method. The relaxation times  $T_{\rm LLS}$  were determined as described in Fig. 1b combined with a four-step phase cycle (Sonnefeld et al., 2022a). The errors correspond to 1 standard deviation. The samples of PFBA, PFBS, and PFPeA had concentrations of 500 mM, all in DMSO-d6.

| Compound                 | νSLIC | $\tau_{ m SLIC}$ | Peak | T <sub>1</sub> [s] at 11.7 T | $T_{\rm LLS}$ [s] at | Ratio $T_{\text{LLS}}/T_1$ | T <sub>1</sub> [s] at 7 T | T <sub>LLS</sub> [s] at | Ratio $T_{\text{LLS}}/T_1$ |
|--------------------------|-------|------------------|------|------------------------------|----------------------|----------------------------|---------------------------|-------------------------|----------------------------|
| Compound                 | [Hz]  | [ms]             | Tour | (470.46 MHz)                 | 11.7 T (470.46 MHz)  | at 11.7 T                  | (282.4 MHz)               | 7 T (282.4 MHz)         | at 7 T                     |
| Perfluorobutanoic        | 574   | 60               | 2    | $0.96 \pm 0.01$              | $3.75 \pm 0.14$      | 3.4                        | $1.67 \pm 0.02$           | $3.17 \pm 0.25$         | 1.9                        |
| acid (PFBA)              | 574   |                  | 3    | $1.62\pm0.02$                | $3.66 \pm 0.16$      | 2.1                        | $2.41 \pm 0.01$           | $3.74 \pm 0.23$         | 1.6                        |
| Perfluorobutane sulfonic |       |                  | 2    | $1.26 \pm 0.0$               | $2.78 \pm 0.07$      | 2.2                        | $2.32 \pm 0.02$           | $5.14 \pm 0.09$         | 2.2                        |
| acid (PFBS)              | 576   | 35               | 3    | $1.21 \pm 0.0$               | $2.92 \pm 0.07$      | 2.4                        | $2.22\pm0.02$             | $4.56 \pm 0.11$         | 2.1                        |
|                          |       |                  | 4    | $1.27\pm0.0$                 | $2.91\pm0.07$        | 2.3                        | $2.31 \pm 0.02$           | $4.59 \pm 0.14$         | 2.0                        |
| Perfluoropentanoic       |       |                  | 2    | $0.69 \pm 0.0$               | $2.24 \pm 0.06$      | 3.2                        | $1.2 \pm 0.01$            | $3.28 \pm 0.25$         | 2.7                        |
| acid (PFPeA)             | 585   | 80               | 3    | $1.04 \pm 0.0$               | $2.23 \pm 0.05$      | 2.1                        | $1.59 \pm 0.02$           | $3.11 \pm 0.32$         | 2.0                        |
|                          |       |                  | 4    | $1.09 \pm 0.0$               | $2.41 \pm 0.07$      | 2.2                        | $1.7 \pm 0.02$            | $2.8 \pm 0.24$          | 1.6                        |

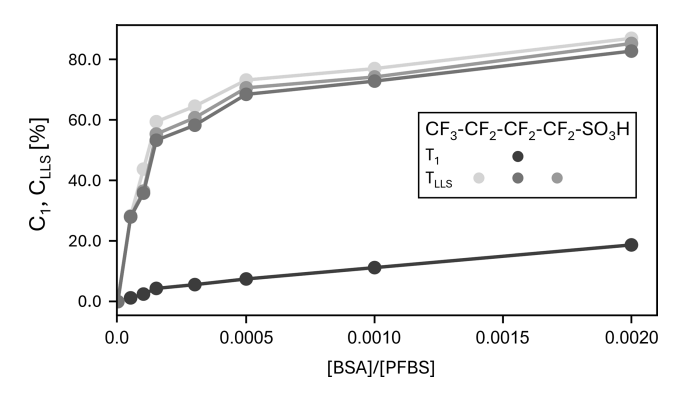


Figure 5.  $T_{\rm LLS}$  and  $T_{\rm 1}$  contrast curves at 11.7 T for eight samples with [PFBS] = 50 mM and 0 < [BSA] < 100  $\mu$ M. The curves showing  $T_{\rm LLS}$  contrast are shown for each of the CF<sub>2</sub> groups, while the  $T_{\rm 1}$  contrast is only shown for the central CF<sub>2</sub> group. The contrast is normalized and expressed as a percentage between 0 % and 100 %. The samples are composed of PFBS, BSA, and a phosphate buffer to obtain solutions of pH  $\approx$  7.2.

longitudinal relaxation, with  $R_1 = 1/T_1$  or  $C_{LLS} = (R_{LLS}^{obs} - R_{LLS}^{free})/R_{LLS}^{obs}$ , with  $R_{LLS} = 1/T_{LLS}$  for experiments measuring long-lived state lifetimes.

As shown in Fig. 5, the relaxation times  $T_{\rm LLS}$  are clearly affected by the binding of the ligand to the target protein. In addition, <sup>19</sup>F LLSs created in PFBS offer good contrast even if the protein is  $10^{-4}$  times more dilute than the ligand. Note that the contrast obtained with  $T_1(^{19}\text{F})$  is much worse than the contrast obtained with  $T_{\rm LLS}(^{19}\text{F})$ . We believe that the contrast can be improved at lower magnetic fields (where the chemical shift anisotropy is less efficient), but we have not yet been able to verify this expectation.

#### 3 Conclusion

It has been shown that for fluorinated aliphatic chains, the amplitudes of forbidden outer singlet-triplet transitions (OSTs) can be boosted in 1-D <sup>19</sup>F NMR spectra, which is crucial for the optimization of SLIC parameters to create long-lived states involving four or six <sup>19</sup>F spins in isotropic solution. We demonstrate that long-lived states of <sup>19</sup>F spins can be readily excited in three different achiral molecules containing fluorinated aliphatic chains. At a field of 11.7 T (470.46 MHz for <sup>19</sup>F, 500 MHz for <sup>1</sup>H), the lifetimes  $T_{\rm LLS}(^{19}{\rm F})$  of the long-lived states exceed the longitudinal relaxation times  $T_1(^{19}F)$  by a factor between 2.1 and 3.4. We also measured  $T_1(^{19}F)$  and  $T_{LLS}(^{19}F)$  lifetimes at a field of 7T (282.4 MHz for <sup>19</sup>F, 300 MHz for <sup>1</sup>H), which were overall longer than those measured at 11.7 T but showed similar ratios of  $T_{LLS}/T_1$ . Fluorinated aliphatic chains can be attached to existing drugs to improve their metabolic or pharmacokinetic properties. This makes the excitation of LLS interesting for drug screening, where it has been demonstrated that LLSs show good contrast when binding to target pro-

**Author contributions.** KS designed the research. CW and SVD performed the experiments and analyzed the data. All authors contributed to writing the paper.

**Competing interests.** At least one of the (co-)authors is a member of the editorial board of *Magnetic Resonance*. The peer-review process was guided by an independent editor, and the authors have no other competing interests to declare.

**Disclaimer.** Publisher's note: Copernicus Publications remains neutral with regard to jurisdictional claims made in the text, published maps, institutional affiliations, or any other geographical rep-

resentation in this paper. While Copernicus Publications makes every effort to include appropriate place names, the final responsibility lies with the authors. Views expressed in the text are those of the authors and do not necessarily reflect the views of the publisher.

**Acknowledgements.** The relaxation rates were measured at two fields at the suggestion of Michael Tayler, who made many other useful comments as reviewer.

Financial support. This work was supported by the European Research Council (ERC)'s Synergy Grant "Highly Informative Drug Screening by Overcoming NMR Restrictions" (Horizon Europe, European Research Council, HISCORE, grant no. 951459). Kirill Sheberstov received support from l'Agence Nationale de la Recherche (ANR) on the project THROUGH-NMR (grant no. ANR-24-CE93-0011-01).

**Review statement.** This paper was edited by Patrick Giraudeau and reviewed by Michael Tayler and one anonymous referee.

#### References

- Aguilar, J. A., Nilsson, M., Bodenhausen, G., and Morris, G. A.: Spin echo NMR spectra without J modulation, Chem. Commun., 48, 811–813, https://doi.org/10.1039/C1CC16699A, 2012.
- Bornet, A., Ji, X., Mammoli, D., Vuichoud, B., Milani, J., Bodenhausen, G., and Jannin, S.: Long-Lived States of Magnetically Equivalent Spins Populated by Dissolution-DNP and Revealed by Enzymatic Reactions, Chem. Eur. J., 20, 17113–17118, https://doi.org/10.1002/chem.201404967, 2014.
- Buchholz, C. R. and Pomerantz, W. C. K.: <sup>19</sup>F NMR viewed through two different lenses: ligand-observed and protein-observed <sup>19</sup>F NMR applications for fragment-based drug discovery, RSC Chem. Biol., 2, 1312–1330, https://doi.org/10.1039/D1CB00085C, 2021.
- Buratto, R., Mammoli, D., Canet, E., and Bodenhausen, G.: Ligand–Protein Affinity Studies Using Long-Lived States of Fluorine-19 Nuclei, J. Med. Chem., 59, 1960–1966, https://doi.org/10.1021/acs.jmedchem.5b01583, 2016.
- Cavadini, S., Dittmer, J., Antonijevic, S., and Bodenhausen, G.: Slow Diffusion by Singlet State NMR Spectroscopy, J. Am. Chem. Soc., 127, 15744–15748, https://doi.org/10.1021/ja052897b, 2005.
- Cheshkov, D. A., Sheberstov, K. F., Sinitsyn, D. O., and Chertkov, V. A.: ANATOLIA: NMR software for spectral analysis of total lineshape, Magn. Reson. Chem., 56, 449–457, https://doi.org/10.1002/mrc.4689, 2018.
- DeVience, S. J., Walsworth, R. L., and Rosen, M. S.: Preparation of Nuclear Spin Singlet States Using Spin-Lock Induced Crossing, Phys. Rev. Lett., 111, 173002, https://doi.org/10.1103/PhysRevLett.111.173002, 2013.
- Dumez, J.-N., Hill-Cousins, J. T., Brown, R. C. D., and Pileio, G.: Long-lived localization in magnetic resonance imaging, J. Magn. Reson. San Diego Calif. 1997, 246, 27–30, https://doi.org/10.1016/j.jmr.2014.06.008, 2014.

- Elliott, S. J., Kadeřávek, P., Brown, L. J., Sabba, M., Glöggler, S., O'Leary, D. J., Brown, R. C. D., Ferrage, F., and Levitt, M. H.: Field-cycling long-lived-state NMR of 15N2 spin pairs, Mol. Phys., 117, 861–867, https://doi.org/10.1080/00268976.2018.1543906, 2019.
- Feng, Y., Theis, T., Liang, X., Wang, Q., Zhou, P., and Warren, W. S.: Storage of Hydrogen Spin Polarization in Long-Lived 13C2 Singlet Order and Implications for Hyperpolarized Magnetic Resonance Imaging, J. Am. Chem. Soc., 135, 9632–9635, https://doi.org/10.1021/ja404936p, 2013.
- Fenton, S. E., Ducatman, A., Boobis, A., DeWitt, J. C., Lau, C., Ng, C., Smith, J. S., and Roberts, S. M.: Per- and Polyfluoroalkyl Substance Toxicity and Human Health Review: Current State of Knowledge and Strategies for Informing Future Research, Environ. Toxicol. Chem., 40, 606–630, https://doi.org/10.1002/etc.4890, 2021.
- Franzoni, M. B., Buljubasich, L., Spiess, H. W., and Münnemann, K.: Long-Lived 1H Singlet Spin States Originating from Para-Hydrogen in Cs-Symmetric Molecules Stored for Minutes in High Magnetic Fields, J. Am. Chem. Soc., 134, 10393–10396, https://doi.org/10.1021/ja304285s, 2012.
- Harbor-Collins, H., Sabba, M., Bengs, C., Moustafa, G., Leutzsch, M., and Levitt, M. H.: NMR spectroscopy of a 18O-labeled rhodium paddlewheel complex: Isotope shifts, 103Rh–103Rh spin–spin coupling, and 103Rh singlet NMR, J. Chem. Phys., 160, 014305, https://doi.org/10.1063/5.0182233, 2024.
- Kiryutin, A. S., Panov, M. S., Yurkovskaya, A. V., Ivanov, K. L., and Bodenhausen, G.: Proton Relaxometry of Long-Lived Spin Order, ChemPhysChem, 20, 766–772, https://doi.org/10.1002/cphc.201800960, 2019a.
- Kiryutin, A. S., Rodin, B. A., Yurkovskaya, A. V., Ivanov, K. L., Kurzbach, D., Jannin, S., Guarin, D., Abergel, D., and Bodenhausen, G.: Transport of hyperpolarized samples in dissolution-DNP experiments, Phys. Chem. Chem. Phys., 21, 13696–13705, https://doi.org/10.1039/C9CP02600B, 2019b.
- Korenchan, D. E., Lu, J., Levitt, M. H., and Jerschow, A.: 31P nuclear spin singlet lifetimes in a system with switchable magnetic inequivalence: experiment and simulation, Phys. Chem. Chem. Phys., 23, 19465–19471, https://doi.org/10.1039/D1CP03085J, 2021.
- Kress, T., Walrant, A., Bodenhausen, G., and Kurzbach, D.: Long-Lived States in Hyperpolarized Deuterated Methyl Groups Reveal Weak Binding of Small Molecules to Proteins, J. Phys. Chem. Lett., https://doi.org/10.1021/acs.jpclett.9b00149, 2019.
- Krivdin, L. B.: Computational aspects of <sup>19</sup>F NMR, Russ. Chem. Rev., 89, 1040–1073, https://doi.org/10.1070/RCR4948, 2020.
- Lorz, N., Czarniecki, B., Loss, S., Meier, B., and Gossert, A. D.: Higher Contrast in 1H-Observed NMR Ligand Screening with the PEARLScreen Experiment, Angew. Chem. Int. Ed., 64, e202423879, https://doi.org/10.1002/anie.202423879, 2025.
- Mamone, S., Rezaei-Ghaleh, N., Opazo, F., Griesinger, C., and Glöggler, S.: Singlet-filtered NMR spectroscopy, Sci. Adv., 6, eaaz1955, https://doi.org/10.1126/sciadv.aaz1955, 2020.
- Melchiorre, G., Giustiniano, F., Rathore, S., and Pileio, G.: Singlet-assisted diffusion-NMR (SAD-NMR): extending the scope of diffusion tensor imaging via singlet NMR, Front. Chem., 11, 1224336, https://doi.org/10.3389/fchem.2023.1224336, 2023.
- Nerella, S. G., Singh, P., Sanam, T., and Digwal, C. S.: PET Molecular Imaging in Drug Development: The

- Imaging and Chemistry Perspective, Front. Med., 9, https://doi.org/10.3389/fmed.2022.812270, 2022.
- Pileio, G. and Ostrowska, S.: Accessing the long-time limit in diffusion NMR: The case of singlet assisted diffusive diffraction *q*-space, J. Magn. Reson., 285, 1–7, https://doi.org/10.1016/j.jmr.2017.10.003, 2017.
- Pileio, G., Hill-Cousins, J. T., Mitchell, S., Kuprov, I., Brown, L. J., Brown, R. C. D., and Levitt, M. H.: Long-Lived Nuclear Singlet Order in Near-Equivalent <sup>13</sup>C Spin Pairs, J. Am. Chem. Soc., 134, 17494–17497, https://doi.org/10.1021/ja3089873, 2012.
- Pileio, G., Dumez, J.-N., Pop, I.-A., Hill-Cousins, J. T., and Brown, R. C. D.: Real-space imaging of macroscopic diffusion and slow flow by singlet tagging MRI, J. Magn. Reson., 252, 130–134, https://doi.org/10.1016/j.jmr.2015.01.016, 2015.
- Razanahoera, A., Sonnefeld, A., Bodenhausen, G., and Sheberstov, K.: Paramagnetic relaxivity of delocalized long-lived states of protons in chains of CH<sub>2</sub> groups, Magn. Reson., 4, 47–56, https://doi.org/10.5194/mr-4-47-2023, 2023.
- Razanahoera, A., Sonnefeld, A., Sheberstov, K., Narwal, P., Minaei, M., Kouřil, K., Bodenhausen, G., and Meier, B.: Hyperpolarization of Long-Lived States of Protons in Aliphatic Chains by Bullet Dynamic Nuclear Polarization, Revealed on the Fly by Spin-Lock-Induced Crossing, J. Phys. Chem. Lett., 15, 9024–9029, https://doi.org/10.1021/acs.jpclett.4c01457, 2024.
- Sabba, M., Wili, N., Bengs, C., Whipham, J. W., Brown, L. J., and Levitt, M. H.: Symmetry-based singlet–triplet excitation in solution nuclear magnetic resonance, J. Chem. Phys., 157, 134302, https://doi.org/10.1063/5.0103122, 2022.
- Salvi, N., Buratto, R., Bornet, A., Ulzega, S., Rentero Rebollo, I., Angelini, A., Heinis, C., and Bodenhausen, G.: Boosting the Sensitivity of Ligand–Protein Screening by NMR of Long-Lived States, J. Am. Chem. Soc., 134, 11076–11079, https://doi.org/10.1021/ja303301w, 2012.
- Sarkar, R., Vasos, P. R., and Bodenhausen, G.: Singlet-State Exchange NMR Spectroscopy for the Study of Very Slow Dynamic Processes, J. Am. Chem. Soc., 129, 328–334, https://doi.org/10.1021/ja0647396, 2007.
- Shah, P. and Westwell, A. D.: The role of fluorine in medicinal chemistry: Review Article, J. Enzyme Inhib. Med. Chem., 22, 527–540, https://doi.org/10.1080/14756360701425014, 2007.
- Sheberstov, K. F., Kiryutin, A. S., Bengs, C., Hill-Cousins, J. T., Brown, L. J., Brown, R. C. D., Pileio, G., Levitt, M. H., Yurkovskaya, A. V., and Ivanov, K. L.: Excitation of singlet-triplet coherences in pairs of nearly-equivalent spins, Phys. Chem. Chem. Phys., 21, 6087–6100, https://doi.org/10.1039/C9CP00451C, 2019a.
- Sheberstov, K. F., Vieth, H.-M., Zimmermann, H., Rodin, B. A., Ivanov, K. L., Kiryutin, A. S., and Yurkovskaya, A. V.: Generating and sustaining long-lived spin states in 15N,15N'-azobenzene, Sci. Rep., 9, 20161, https://doi.org/10.1038/s41598-019-56734-y, 2019b.

- Sheberstov, K. F., Sonnefeld, A., and Bodenhausen, G.: Collective long-lived zero-quantum coherences in aliphatic chains, J. Chem. Phys., 160, 144308, https://doi.org/10.1063/5.0196808, 2024.
- Sicoli, G., Sieme, D., Overkamp, K., Khalil, M., Backer, R., Griesinger, C., Willbold, D., and Rezaei-Ghaleh, N.: Large dynamics of a phase separating arginine-glycine-rich domain revealed via nuclear and electron spins, Nat. Commun., 15, 1610, https://doi.org/10.1038/s41467-024-45788-w, 2024.
- Sonnefeld, A., Bodenhausen, G., and Sheberstov, K.: Polychromatic Excitation of Delocalized Long-Lived Proton Spin States in Aliphatic Chains, Phys. Rev. Lett., 129, 183203, https://doi.org/10.1103/PhysRevLett.129.183203, 2022a.
- Sonnefeld, A., Razanahoera, A., Pelupessy, P., Bodenhausen, G., and Sheberstov, K.: Long-lived states of methylene protons in achiral molecules, Sci. Adv., 8, eade2113, https://doi.org/10.1126/sciadv.ade2113, 2022b.
- Stevanato, G., Hill-Cousins, J. T., Håkansson, P., Roy, S. S., Brown, L. J., Brown, R. C. D., Pileio, G., and Levitt, M. H.: A Nuclear Singlet Lifetime of More than One Hour in Room-Temperature Solution, Angew. Chem. Int. Ed., 54, 3740–3743, https://doi.org/10.1002/anie.201411978, 2015.
- Takegoshi, K., Ogura, K., and Hikichi, K.: A perfect spin echo in a weakly homonuclear J-coupled two spin- system, J. Magn. Reson. 1969, 84, 611–615, https://doi.org/10.1016/0022-2364(89)90127-3, 1989.
- Tayler, M. C. D.: Filters for Long-lived Spin Order, in: New Developments in NMR, Royal Society of Chemistry, 188–208, https://doi.org/10.1039/9781788019972-00188, 2020.
- Tayler, M. C. D., Marco-Rius, I., Kettunen, M. I., Brindle, K. M., Levitt, M. H., and Pileio, G.: Direct Enhancement of Nuclear Singlet Order by Dynamic Nuclear Polarization, J. Am. Chem. Soc., 134, 7668–7671, https://doi.org/10.1021/ja302814e, 2012.
- Tourell, M. C., Pop, I.-A., Brown, L. J., Brown, R. C. D., and Pileio, G.: Singlet-assisted diffusion-NMR (SAD-NMR): redefining the limits when measuring tortuosity in porous media, Phys. Chem. Chem. Phys., 20, 13705–13713, https://doi.org/10.1039/C8CP00145F, 2018.
- Vasos, P. R., Comment, A., Sarkar, R., Ahuja, P., Jannin, S., Ansermet, J.-P., Konter, J. A., Hautle, P., van den Brandt, B., and Bodenhausen, G.: Long-lived states to sustain hyperpolarized magnetization, Proc. Natl. Acad. Sci., 106, 18469–18473, https://doi.org/10.1073/pnas.0908123106, 2009.
- Zhao, L., Teng, M., Zhao, X., Li, Y., Sun, J., Zhao, W., Ruan, Y., Leung, K. M. Y., and Wu, F.: Insight into the binding model of per- and polyfluoroalkyl substances to proteins and membranes, Environ. Int., 175, 107951, https://doi.org/10.1016/j.envint.2023.107951, 2023.